

# Rapid viscoelastic switching of an ambient temperature range photo-responsive azobenzene side chain liquid crystal polymer

Michael Petr,<sup>a</sup> Matthew E. Helgeson,<sup>a</sup> Johannes Soulages,<sup>b</sup> Gareth H. McKinley,<sup>b</sup> and Paula T. Hammond\*<sup>a</sup>

<sup>a</sup> Department of Chemical Engineering, Massachusetts Institute of Technology, Cambridge, MA 02139, USA

<sup>b</sup> Department of Mechanical Engineering, Massachusetts Institute of Technology, Cambridge, MA 02139, USA

## ARTICLE INFO

### Article history:

Received

Received in revised form

date

Accepted

Available

### Keywords:

Photo-responsive

Liquid Crystal Polymer

Small Amplitude Oscillatory Shear

## ABSTRACT

We report the rheological properties of a new azobenzene side chain liquid crystal polymer (SCLCP) with photo-responsive behavior in the range of 0°C to 50°C as probed by small amplitude oscillatory shear (SAOS) rheometry with *in situ* UV irradiation. In the linear viscoelastic (LVE) strain regime, temperature sweeps measured  $G'$  and  $G''$  from 80°C to -5°C and identified glass transition temperatures ( $T_g$ ) at 2.2°C and 0.3°C for UV-off and UV-on, respectively. Also in the LVE strain regime, frequency sweeps identified  $G'$  and  $G''$  cross-over frequencies at 5°C and 0°C. Most importantly, rapid shear modulus changes of between 7-35% were demonstrated at 50°C, 25°C, 5°C, and 0°C by successively turning the UV light on and off during time sweeps in the LVE strain regime. The elastic ( $G'$ ) and viscous ( $G''$ ) shear moduli reversibly decreased by a maximum of 35% and 21%, respectively, with time constants ( $\tau$ ) from 6 s to 18 s as fit by a stretched exponential model. This significant, rapid, and reversible UV-triggered modulus switching at temperatures as low as 0°C and up to 50°C is noteworthy because it represents a bulk property change at temperatures that are in the ambient range for several geographic regions and has reasonable time constants across the range.

## 1. Introduction

Photo-responsive materials have gained interest for their ability to change properties by merely irradiating them with the correct wavelength of light in the appropriate temperature range. Of particular interest are photo-responsive azobenzene liquid crystal polymers (LCP), which are the most common of this class of materials.[1, 2] The azobenzene moiety is a robust, reliable, and reversible chromophore that is well understood, and can be used as part of the LC moiety of an LCP. Liquid crystal polymers are useful because the photo-induced LC to isotropic phase transition provides the photo-response, and the polymer provides a permanent network structure and mechanical stability.

It is these properties that make azobenzene LCPs attractive as photo-responsive materials.[2-4] However, the quick, reversible, and large responses required for such applications have only been achieved at elevated temperatures or with relatively slow response times.[5-7] These responses are slow at room temperature because the glass transition temperature ( $T_g$ ) of the polymer and/or the isotropization temperature ( $T_{iso}$ ) of the LC are well above room temperature. There have been two approaches to circumvent this problem to obtain room temperature, rapid, and reversible photo-responses. The first is replacement of the azobenzene pendant group with a dissolved azobenzene chromophore. This technique has been used to prepare crosslinked nematic azobenzene polysiloxane thin films with response times ranging from milliseconds to seconds, depending on the irradiation intensity used.[8, 9] A second approach involves complex alignment, mounting, and movement of the azobenzene LCP in conjunction with a high-powered polarized light source. Using this method, thin films and cantilevers of aligned crosslinked nematic azobenzene polyacrylates have shown very fast response rates, although they require relatively large light intensities.[10, 11] However, these solutions are not practical under all circumstances. For example, in the first technique, the azobenzene moiety is no longer chemically linked and, therefore, requires specific processing strategies, and it cannot be used under conditions that interfere or change this processing. In the second technique, the glass transition temperature limitation was overcome by the use of a strong polarized laser and a complicated irradiation geometry and procedure.

A more general solution to obtain a robust, rapid, and reversible photo-responsive material would be an azobenzene LCP with a low glass transition temperature and a low isotropization temperature.[12] Previously, we have synthesised a new azobenzene side-on side chain (SC) nematic LC polysiloxane that is such a material with a glass transition temperature of -7°C and an isotropization temperature of 73°C.[13] In the present work, we extend this previous study by performing rheological characterization of this material by small amplitude oscillatory shear (SAOS) rheometry with *in situ* UV irradiation. This provides complete characterization of the viscoelastic properties of the polymer, demonstrating that its photo-responsive behavior is, in fact, rapid, significant, and reversible over a substantial temperature range from well below room temperature to well above room temperature. This represents an improvement over current systems because it takes place in the bulk at ambient conditions and requires only a moderate intensity UV light

source.

## 2. Experimental

### 2.1 Materials

The material used in the study was a photo-responsive nematic side chain liquid crystal polymer. Its synthesis was reported previously.[13]

### 2.2 Instrumentation

Small Amplitude Oscillatory Shear (SAOS) was performed on a Rheometrics ARES strain-controlled rheometer using a parallel plate geometry. The bottom plate was made of copper with a thin chromium-based coating by Micro-E, Electroforming Inc., and its temperature was controlled by an ARES Peltier control system. The upper plate was an ARES UV Curing accessory, which consists of a 20 mm diameter transparent quartz plate. The plate is housed within a tube containing a 45° mirror onto which light is incident and transmitted to the sample. *In situ* UV irradiation was carried out with a Dymax Blue Wave 200 source with a Thorlabs, Inc. FGUV W53199 UV filter. Finally, UV light intensity was measured with a Dymax ACCU-CAL 50 radiometer.

### 2.3 Procedure

After set-up of the equipment, the UV light was aligned with the mirror on the upper rheometer plate at a gap large enough for the radiometer head to fit (~4 mm), and the intensity of the UV light transmitted through the quartz plate was measured at 125 mW/cm<sup>2</sup>. The gap was then set to around 0.2 mm, and the UV light was re-aligned. Next, approximately 80 mg of crystalline LCP was placed on the bottom plate at room temperature. The plate was then heated to 80°C for several minutes and sheared to completely melt the crystalline phase of the LCP. Subsequently, the gap was set to 0.28 mm in order to completely fill the parallel plate geometry with the nematic phase, which is less dense than the crystal phase. Prior to measurement, auto-tension as well as manual gap adjustment were used to minimize tension or compression on the sample. Finally, a series of temperature sweeps, time sweeps, amplitude sweeps, frequency sweeps, and SAOS experiments, all with UV-off and with UV-on, were performed.

## 3. Results and discussion

### 3.1 Thermal and Temporal Effects

With the LVE strain regime established within the functional temperature range of the material (see Appendix A, Supplementary material for details), thermal and temporal characterization was performed with temperature and frequency sweeps, respectively. In Fig. 1, temperature sweep data is reported with the UV source both off and on from -5 °C to 80 °C at 5 °C/min at an applied frequency and strain amplitude of 10 rad/s and 1%, respectively. Even though 1% strain was commanded, the actual strain attained at the lowest temperatures was reduced because of instrument compliance. The data in Fig.

\* Corresponding authors.

E-mail addresses: hammond@mit.edu.

1a exhibits shear storage ( $G'$ ) and loss ( $G''$ ) moduli which vary by six orders of magnitude over temperatures ranging from the glass transition temperature to the isotropization temperature due to the concomitant increase in free volume of the LCP. At temperatures above 55 °C, the material exhibits soft viscoelastic solid-like behavior with constant values for  $G'$  and  $G''$  and with  $G' < G''$ . [14] In this regime, the difference in  $G''$  between UV-off and UV-on is quite small, due to the decreased order in the nematic phase near the isotropization temperature. [15] Between 55°C and around 2°C, the polymer is a viscoelastic fluid, but as the temperature approaches the glass transition, the material becomes gel-like as it begins to form “preglassy elastic clusters,” [14] and ultimately the moduli increase by 4 orders of magnitude (Fig. 1a), much as described for other LC elastomers. This behavior coincides with the glass transition observed for the polymer in our previous work [13] and is consistent with previously reported data on siloxane based LC homopolymers. [15-17] At room temperature and below, a significant difference in moduli between UV-off and UV-on develops (Fig. 1b). These differences in  $G'$  and  $G''$  achieve

maximal values of 44% and 23% at 4.7°C and 5.6°C, respectively. In this temperature range, a crossover with  $G' > G''$  is observed with decreasing temperature as the material transitions to a glassy response. Defining the glass transition as the crossover in  $G'$  and  $G''$ , the values for the glass transition temperature are 2.2 °C and 0.3 °C for UV-off and UV-on, respectively. At even lower temperatures  $G''$  goes through a maximum at 0.6°C and -1.6°C for UV-off and UV-on, respectively, and decreases as the material is cooled further. These results show that UV light significantly decreases the isotropization temperature of the LCP so that, under ambient temperature conditions, the application of UV light destroys the nematic phase and decreases the rigidity of the LCP. [13] Finally, below -2.5°C, the difference between  $G'$  for UV-off and UV-on again vanishes, demonstrating that, below the glass transition temperature, the polymer chains are insufficiently mobile to rearrange upon UV irradiation.

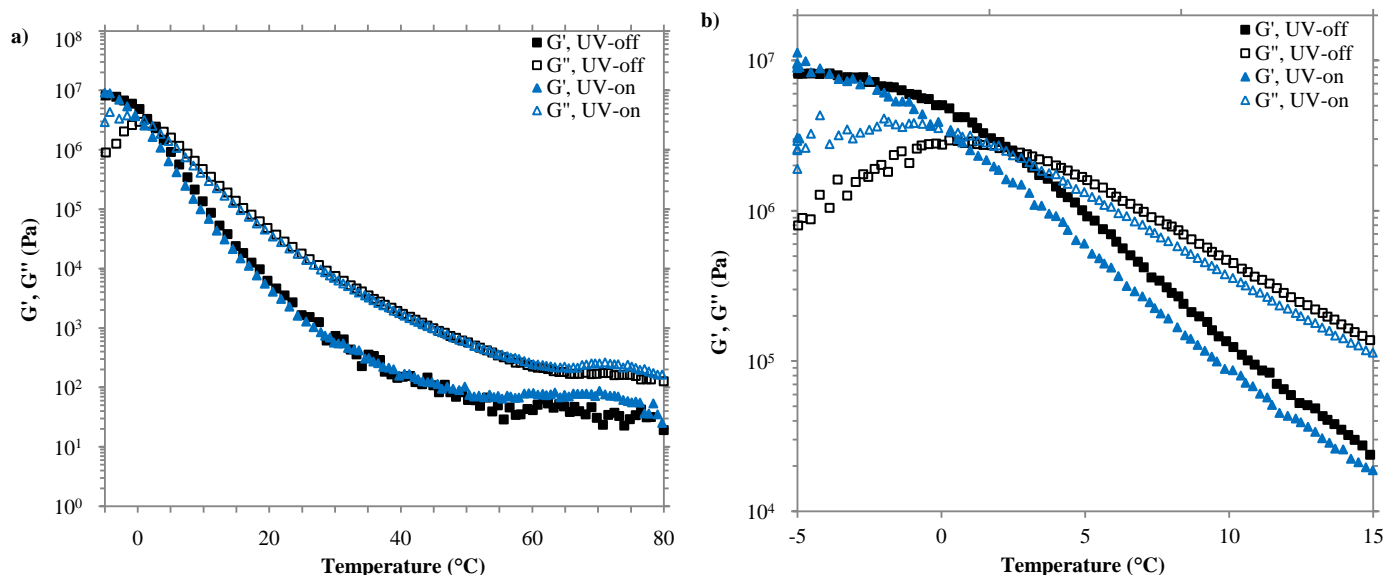


**Fig. 1.** Temperature sweeps with both UV-off and UV-on at 5°C/min, 10 rad/s, and 1% commanded strain a) from 80°C to -5°C and b) zoomed in from 15°C to -5°C. In a), only every fifth point is shown, but in b), every point is shown.

The results of the temporal characterization are consistent with that of the thermal characterization and the principle of time-temperature superposition. [18] Fig. 2 shows a series of frequency sweeps in the LVE strain regime at a) 50°C, b) 25°C, c) 5°C, and d) 0°C for both UV-off and UV-on. At 50°C and 25°C and above 1 rad/s,  $G'$  and  $G''$  for UV-off and UV-on exhibit power law behavior, as in eqn (1)

$$G = S\omega^n \quad (1)$$

where  $\omega$  is the frequency of oscillation and  $S$  and  $n$  are the prefactor and exponent, respectively, of the linearized fit on log-log axes. Table 1 lists the parameters from all of the power law fits. The slopes and intercepts for UV-off and UV-on were almost identical; however, temperature affected the slopes for the elastic modulus,  $G'$ . At 50°C the slopes were below unity, characteristic of a power law physical gel. As the temperature was lowered, the slopes steadily increased and passed through unity, as in the slopes at 25°C; however, the terminal regime is not attained within the accessible frequency range. On the other hand, all the slopes for  $G''$  were close to unity, as expected for a viscoelastic liquid. As the temperature continued to decrease toward the glass transition temperature, as in Fig. 2c,  $G'$  and  $G''$  for UV-off and UV-on still

increased qualitatively as power laws at low frequencies but began to gradually level off at high frequencies, indicative of a distribution of relaxation time constants. [19] In addition,  $G''$  was observed to pass through a maximum at 50 rad/s and 63 rad/s for UV-off and UV-on, respectively, and the material itself goes through a glass transition of sorts, where  $G'$  and  $G''$  cross, at 32 rad/s and 50 rad/s for UV-off and UV-on, respectively. Finally, Fig. 2d at 0°C shows all the same trends as Fig. 2c but shifted to lower frequencies because of the lower free volume in which the chains can rearrange upon deformation. There are the low frequency power law increases in  $G'$  and  $G''$ , the higher frequency levelling off of  $G'$  and  $G''$ , again indicative of a distribution of relaxation time constants, a maximum in the loss modulus  $G''$  at 7.9 rad/s for both UV-off and UV-on, and the cross-over frequency at 4.0 rad/s and 6.3 rad/s for UV-off and UV-on, respectively. It is important to note that the cross-over frequency is greater than 10 rad/s at 5°C and less than 10 rad/s at 0°C because a test frequency of 10 rad/s was the condition used in Fig. 1 and Fig. 5 as well as in the LVE strain sweep characterization (see Appendix A, Supplementary material for details); this is why the frequency-dependent glass transition temperature observed by SAOS was between 0°C and 5°C.

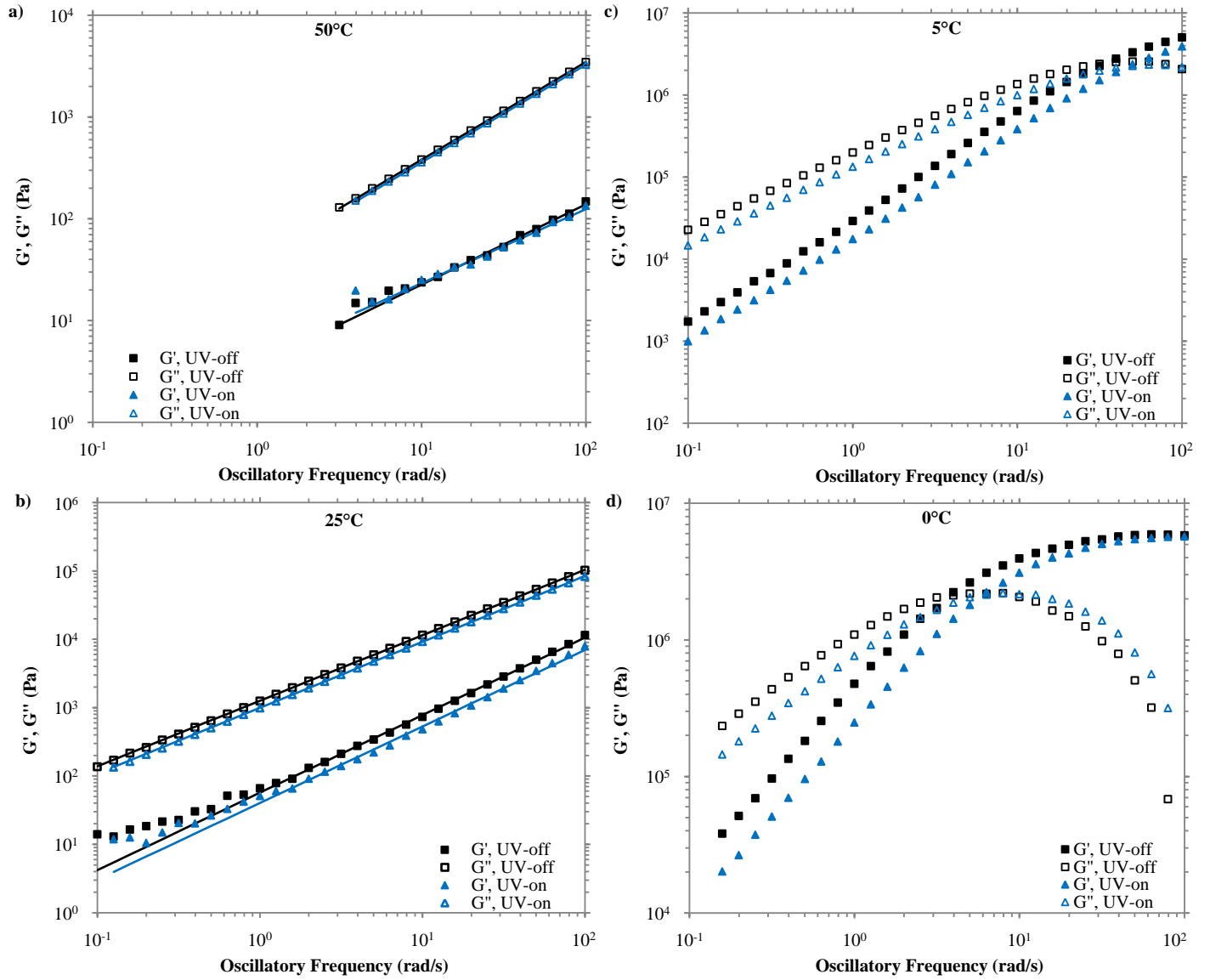


Fig. 2. Frequency sweeps with both UV-off and UV-on in the LVE strain regime (see Appendix A, Supplementary material for details) at a) 50°C, b) 25°C, c) 5°C, and d) 0°C. The filled lines in a) and b) are the power law fits with eqn (1), and the corresponding parameters are in Table 1.

Table 1  
G' and G'' power law fit parameters for 50°C and 25°C.

		50°C		25°C	
		UV-off	UV-on	UV-off	UV-on
G'	S'	3.66	4.36	57.1	40.3
	n'	0.789	0.728	1.13	1.12
G''	S''	41.8	39.2	1264	997
	n''	0.959	0.960	0.958	0.964

### 3.2 Time-Temperature Superposition

To further demonstrate the equivalent thermal and temporal effects, time-temperature superposition was performed with the frequency sweeps in Fig. 2 to produce Fig. 3. G' and G'' were shifted manually with a single shift factor to 25°C for both UV-off and UV-on, and these shift factors are shown in Fig. 4. They were then fit with the Williams-Landel-Ferry (WLF) equation shown in eqn (2) [18]

$$\log a_T = \frac{-C_1(T - T_{ref})}{C_2 + (T - T_{ref})} \quad (2)$$

where  $a_T$  is the shift factor at temperature T in °C,  $C_1$  and  $C_2$  are the WLF constants, and  $T_{ref}$  is the reference temperature to which the data is shifted. To compare to other polymers, these 25°C WLF constants can be mathematically transformed to correspond with the UV-off and UV-on glass transition temperature of the LCP using eqn (3) and eqn (4)

$$C_1' = C_1 + \log a_{T_g} \quad (3)$$

$$C_2' = C_2 + (T_g - T_{ref}) \quad (4)$$

where  $C_1'$  and  $C_2''$  are the transformed WLF constants. Table 2 lists all the WLF constants as well as the glass transition temperatures from Fig. 1 and the shift factors used in the calculations. Compared to other polymers,  $C_1'$  is in between that of polydimethylsiloxane (PDMS) and the universal value of  $C_1'$ , which are 6.1 and 17.44, respectively, and  $C_2'$  is below that of PDMS and very slightly below the universal  $C_2'$ , which are 69 and 51.6, respectively.[20]

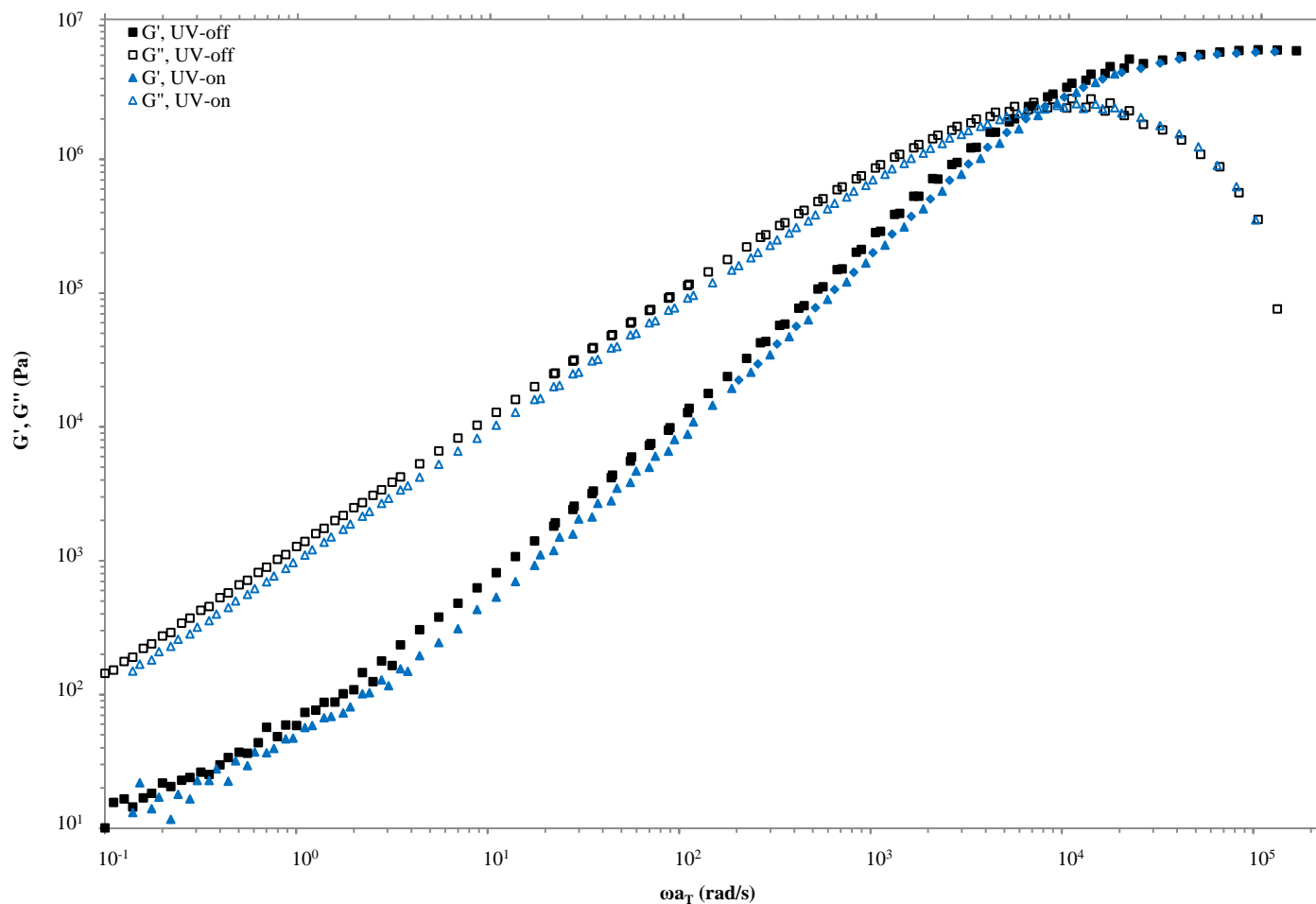


Fig. 3. Time-temperature superposition of frequency sweeps manually shifted to a reference temperature of 25°C.

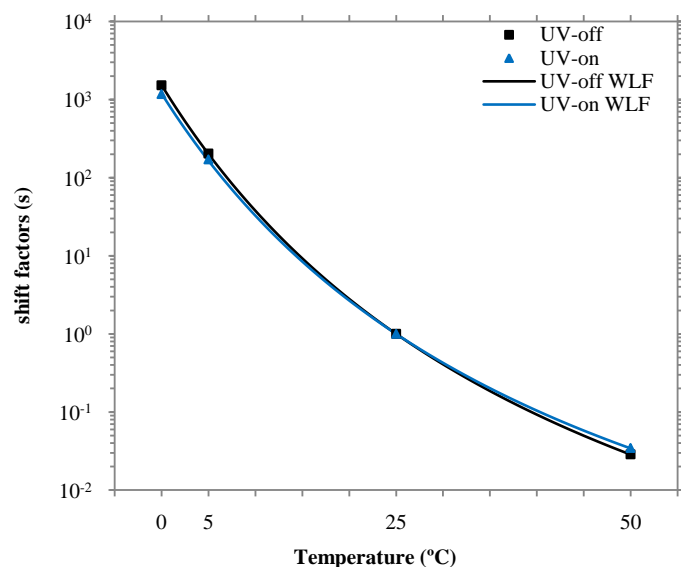


Fig. 4. Shift factors from time-temperature superposition of frequency sweeps fit with the WLF equation in eqn (2).

Table 2 WLF parameters at 25°C from fitting of shift factors in Fig. 4 and WLF parameters translated to the glass transition temperature.

	$T_{ref} = 25^\circ\text{C}$		$T_{ref} = T_g$	
	UV-off	UV-on	UV-off	UV-on
$C_1$	6.00	5.60	8.77	8.62
$C_2$	72.2	70.5	49.4	45.9
$T_g$	2.2	0.3	2.2	0.3
$\log a_{T_g}$	2.77	3.01	0	0

### 3.3 UV switching kinetics

With an understanding of the linear viscoelastic behavior of the material and the effects of the photo-responsive behavior on the temperature-dependent rheology, transient measurements involving UV switching were performed to understand the temporal characteristics of the photo-responsive behavior. Fig. 5 shows a series of time sweeps within the LVE strain regime at 10 rad/s and a) 60°C, b) 50°C, c) 25°C, d) 5°C, e) 0°C, and f) -5°C. Throughout each time sweep, the UV light was successively turned on and off, as indicated by the arrows in Fig. 5, to observe the modulus switching. The data at 60°C and at -5°C shows no discernible response in  $G'$  or  $G''$  to UV light because the material is too close to the isotropization temperature and the glass transition temperature, respectively, of the material. At these conditions the torque and the strain approach the lower and upper limits of the rheometer, respectively, as illustrated by the large amount of scatter in the data. On the other hand, the data at all of the temperatures in between shows a distinct, measurable response in  $G'$  and/or  $G''$ . In particular,  $G''$  decreases significantly upon UV irradiation at 25°C, and both  $G'$  and  $G''$  show their largest decreases of 35% and 21%, respectively, at 5°C. This observation is in good accordance with the

temperature sweeps in Fig. 1, which also show maximum modulus differences around 5°C. Moving to the lowest responsive temperature, we note a particularly interesting feature of the response at 0°C.  $G'$  decreases significantly upon UV irradiation, just as at the other temperatures, but  $G''$  increases slightly. However, this can be rationalized by considering the previous thermal characterization. The complex shear modulus ( $G^*$ ) still decreases, but the contribution from  $G''$  increases because the test temperature

is slightly below the glass transition temperature of the UV-off material but slightly above the glass transition temperature of the UV-on material, shown in Fig. 1. Therefore, at 0°C, UV irradiation shifts the material from a predominantly viscoelastic solid-like character toward a more liquid-like response.

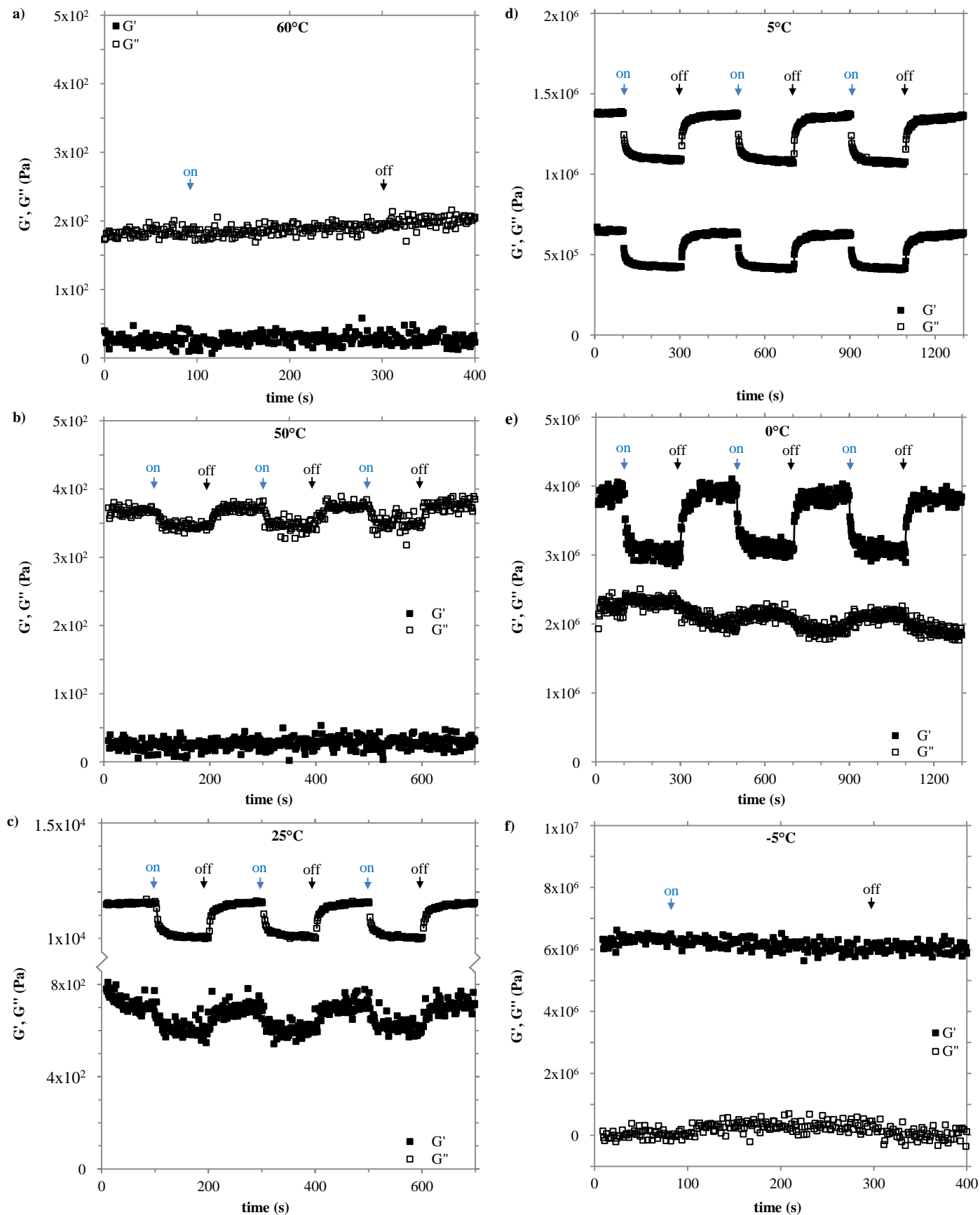


**Fig. 5.** Time sweeps with UV modulus switching in the LVE strain regime at 10 rad/s and a) 60°C, b) 50°C, c) 25°C, d) 5°C, e) 0°C, and f) -5°C. The UV light was initially off at 0 seconds and successively switched on and off again. Blue arrows indicate when the UV light was turned on, and black arrows indicate when the UV light was turned back off. Also, note in c) that  $G'$  and  $G''$  are on different scales, so there is a break in the  $G'$ ,  $G''$  axis.

The final aspect of the UV modulus switching studied is the kinetics with which the transition occurs. UV irradiation lowers  $G'$  and  $G''$  because the *trans* to *cis* isomerization of the azobenzene destabilizes the nematic phase of the polydomain polymer; [15] therefore, the kinetics are characteristic of a distribution of time constants. We describe the switching response of the viscoelastic moduli with the stretched exponential [15] given in eqn (5):

$$\frac{G(t) - G_f}{G_i - G_f} = \exp\left(-\left(\frac{t - t_s}{\tau}\right)^n\right) \quad (5)$$

where  $G$  denotes either  $G'$  or  $G''$ ,  $G_f$  is the steady state modulus long after the UV switch,  $G_i$  is the initial modulus before the UV switch,  $t - t_s$  is the elapsed time since the UV switch,  $\tau$  is the time constant of the photo-responsive transition, and  $n$  is the stretch factor. The data in Fig. 5 was fit to eqn (5), as follows. First,  $G'$  and  $G''$  were averaged from the last 10 s before each UV switch. Second, each switch event was fit with  $\tau$ ,  $n$ , and  $t_s$  as adjustable parameters because the switching was done manually. Third, at each temperature, the data was split into three UV-on segments and three UV-off segments. Fourth, the three UV-on segments were re-fit for overall  $\tau_{on}$  and  $n_{on}$  values keeping the  $t_s$  values obtained from the original fitting, and the three UV-off segments were re-fit for overall  $\tau_{off}$  and  $n_{off}$  values keeping the  $t_s$  values obtained from the original fitting. The results of this fitting, in Fig. 6, demonstrate how fast the modulus switching occurs. Both the  $\tau_{on}$  and  $\tau_{off}$  values are on the order of seconds at room temperature compared to previously reported values for similar systems which are minutes to hours, even at

elevated temperatures. [1, 2, 15] The time constant  $\tau_{on}$  is less than the time constant  $\tau_{off}$  at all temperatures because the UV-on reaction is photo-driven but the UV-off reaction is thermally-driven. Moreover, the  $\tau$  values are initially large at 50°C and then decrease at 25°C and 5°C before increasing again at 0°C because, mathematically, the  $\tau$  values are higher but the  $n$  values are smaller at lower temperatures. As for the  $n$  values in Fig. 6b, they are highest and closest to unity at 50°C with  $n_{on} = 1.18$  and  $n_{off} = 0.78$ , signifying a narrow distribution of time constants. However, they subsequently drop to between 0.38 to 0.54 at the lower temperatures, which is similar to other nematic LCPs, [15] signifying a larger distribution of time constants and reflecting the large distribution of time constants in the frequency sweeps at these temperatures. Because the breadth of the distribution is changing, the average time constant of the distribution, rather than the time constant  $\tau$  from the fit, should be used to compare the time constants at different temperatures. This average time constant was calculated using the following expression: [21]

$$\langle \tau \rangle = \frac{\tau}{n} \Gamma\left(\frac{1}{n}\right) \quad (6)$$

where  $\langle \tau \rangle$  is the average value of the distribution of time constants. In Fig. 7, we show that the average value  $\langle \tau_{on} \rangle$  is still less than  $\langle \tau_{off} \rangle$ , but both  $\langle \tau_{on} \rangle$  and  $\langle \tau_{off} \rangle$  increase monotonically with decreased temperature.

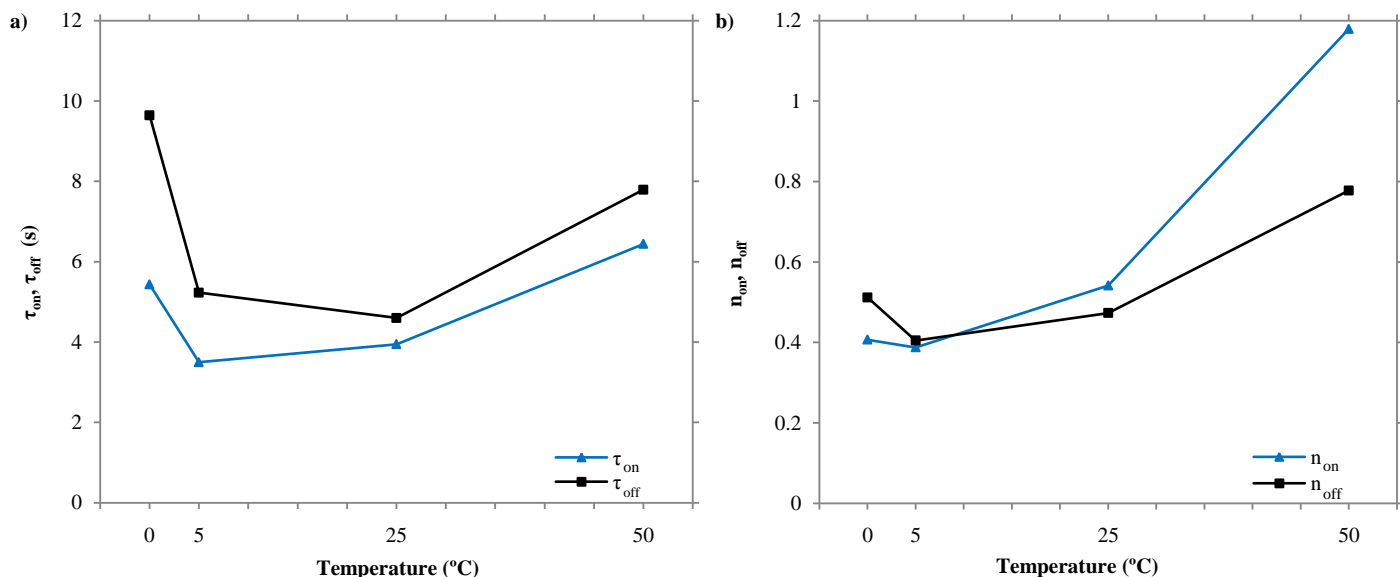


**Fig. 6.** Stretched exponential a) time constant and b) stretch factor parameter values from fitting of moduli cycles in UV switching experiments.  $\tau_{on}$  and  $n_{on}$  correspond to the moduli drops when the UV light was turned on, and  $\tau_{off}$  and  $n_{off}$  correspond to the moduli recoveries when the UV light was turned back off. The points have been connected to aid the eye.

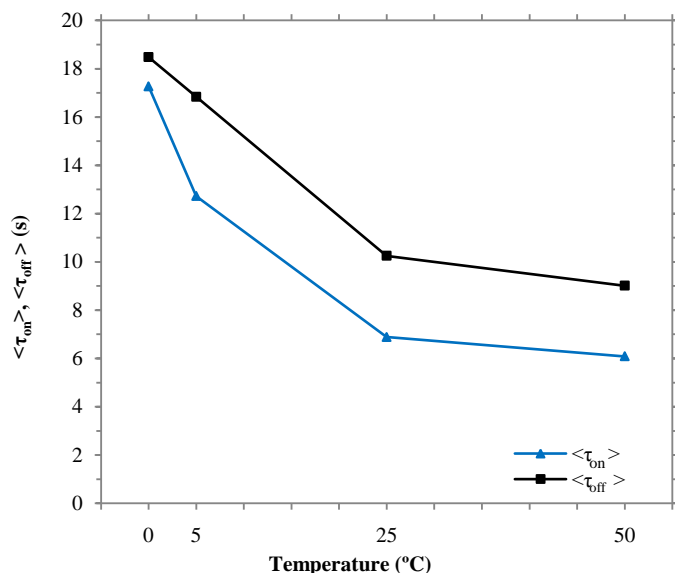


Fig. 7. Average time constants for UV-activation and thermal deactivation calculated using eqn (6) from the stretched exponential fitting of moduli cycles in UV switching experiments.

#### 4. Conclusion

The new Side-Chain Liquid Crystalline Polymer (SCLCP) and its photo-responsive behavior have been characterized by Small Amplitude Oscillatory Shear Flow (SAOS) with in-situ UV irradiation. Temperature and frequency sweeps were used to observe the time-temperature relaxation response of the material, and time sweeps with in-situ UV switching demonstrated that  $G'$  and  $G''$  changed rapidly, significantly, and reversibly upon UV irradiation from 0°C to 50°C. This temperature range is important because it is the ambient temperature for several geographic regions, and this new SCLCP material represents an advancement over other photo-responsive materials because of the significantly more rapid bulk photo-response.

#### Acknowledgements

The authors of this paper would like to thank the U.S. Army Research Office for financial support of this research under contract W911NF-07-D-0004.

#### Appendix A. Supplementary material

Supplementary material related to this article can be found, in the online version, at <http://dx.doi.org/10.1016/j.polymer>.

#### References

- [1] Ohm C, Brehmer M, and Zentel R. *Advanced Materials* 2010;22(31):3366-3387.
- [2] Yu HF and Ikeda T. *Advanced Materials* 2011;23(19):2149-2180.
- [3] Zentel R, Ohm C, and Brehmer M. *Advanced Materials* 2010;22(31):3366-3387.
- [4] Barrett CJ, Mamiya JI, Yager KG, and Ikeda T. *Soft Matter* 2007;3(10):1249-1261.
- [5] Finkelmann H, Nishikawa E, Pereira GG, and Warner M. *Physical Review Letters* 2001;87(1).
- [6] Li MH, Keller P, Li B, Wang XG, and Brunet M. *Advanced Materials* 2003;15(7-8):569-572.
- [7] Verploegen E, Soulages J, Kozberg M, Zhang T, McKinley G, and Hammond P. *Angewandte Chemie-International Edition* 2009;48(19):3494-3498.
- [8] Camacho-Lopez M, Finkelmann H, Palfy-Muhoray P, and Shelley M. *Nature Materials* 2004;3(5):307-310.
- [9] Harvey CLM and Terentjev EM. *European Physical Journal E* 2007;23(2):185-189.
- [10] White TJ, Serak SV, Tabiryan NV, Vaia RA, and Bunning TJ. *Journal of Materials Chemistry* 2009;19(8):1080-1085.
- [11] White TJ, Tabiryan NV, Serak SV, Hrozhyk UA, Tondiglia VP, Koerner H, Vaia RA, and Bunning TJ. *Soft Matter* 2008;4(9):1796-1798.
- [12] Velasco D, Garcia-Amoros J, Pinol A, and Finkelmann H. *Organic Letters* 2011;13(9):2282-2285.
- [13] Petr M and Hammond PT. *Macromolecules* 2011;44(22):8880-8885.
- [14] Pozo O, Collin D, Finkelmann H, Rogez D, and Martinoty P. *Physical Review E* 2009;80(3).
- [15] Sanchez-Ferrer A, Merekalov A, and Finkelmann H. *Macromolecular Rapid Communications* 2011;32(8):671-678.
- [16] Garcia-Amoros J, Finkelmann H, and Velasco D. *Journal of Materials Chemistry* 2011;21(4):1094-1101.
- [17] Verploegen E, Zhang T, Murlo N, and Hammond PT. *Soft Matter* 2008;4(6):1279-1287.
- [18] Sperling LH. *Introduction to physical polymer science*, 3rd ed. New York: Wiley-Interscience, 2001.
- [19] DeRosa ME, Adams WW, Bunning TJ, Shi HQ, and Chen SW. *Macromolecules* 1996;29(17):5650-5657.
- [20] Ferry J. *Viscoelastic properties of polymers*, 3d ed. New York: Wiley, 1980.
- [21] Laviolette M, Auger M, and Desilets S. *Macromolecules* 1999;32(5):1602-1610.



# Rapid viscoelastic switching of an ambient temperature range photo-responsive azobenzene side chain liquid crystal polymer

Michael Petr,<sup>a</sup> Matthew E. Helgeson,<sup>a</sup> Johannes Soulages,<sup>b</sup> Gareth H. McKinley,<sup>b</sup> and Paula T. Hammond\*<sup>a</sup>

<sup>a</sup> Department of Chemical Engineering, Massachusetts Institute of Technology, Cambridge, MA 02139, USA

<sup>b</sup> Department of Mechanical Engineering, Massachusetts Institute of Technology, Cambridge, MA 02139, USA

## S1. Results and discussion

### S1.1 Small Amplitude Oscillatory Shear Conditions

The photo-responsive nematic side chain liquid crystal polymer is shown in Fig. S1. It contains an azobenzene and benzoate moiety, whose thermodynamically favored *trans* conformation imparts liquid crystalline behaviour. In addition, the material shows a glass transition temperature ( $T_g$ ), a melting temperature ( $T_m$ ), and a nematic to isotropic transition temperature ( $T_{iso}$ ) of 7°C, 42°C, and 73°C, respectively, as measured by Differential Scanning Calorimetry (DSC).[13] After loading the sample, annealing at 80°C followed by a pre-shear step was used to melt and break up the initial crystalline phase. Fortunately, this crystalline phase takes at least several days to form at room temperature; therefore, the material was tested in its nematic or metastable nematic phase, which, in principle, exists from  $T_g$  to  $T_{iso}$ . [13]

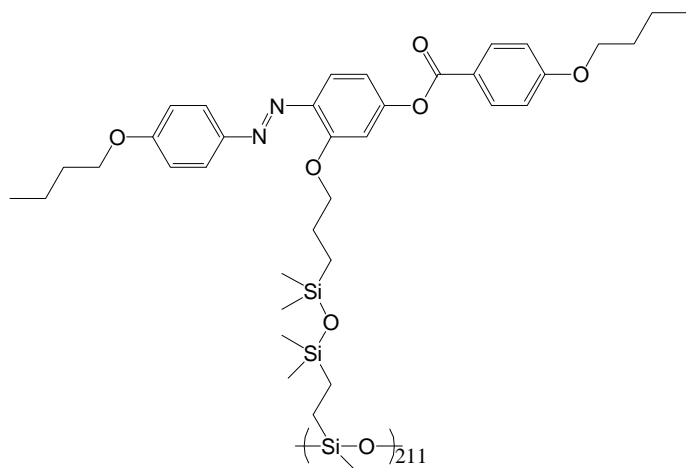


Fig. S1. Structure of the photo-responsive nematic SCLCP in the SAOS experiments.

Parallel plate SAOS with in situ UV irradiation, a schematic of which is shown in Fig. S2, was a convenient way to observe the reversible modulus switching in real time. The azobenzene moiety in Fig. S2, whose *trans* to *cis* isomerization, upon absorption of a UV photon, provides its photo-responsive behavior. The UV light intensity penetrating the upper quartz plate to the top of the sample was 125 mW/cm<sup>2</sup>, which was more than enough to execute the nematic to isotropization quickly. With the exception of the time sweeps, where the kinetics of isotropization were measured, the various UV-off and UV-on tests were separated by several minutes in order to ensure the isotropization had reached steady state. Since illumination is controlled independently of the rheometer, the sample temperature as well as the other experimental parameters were easily controlled without having to interchange any fixtures or reload the sample.

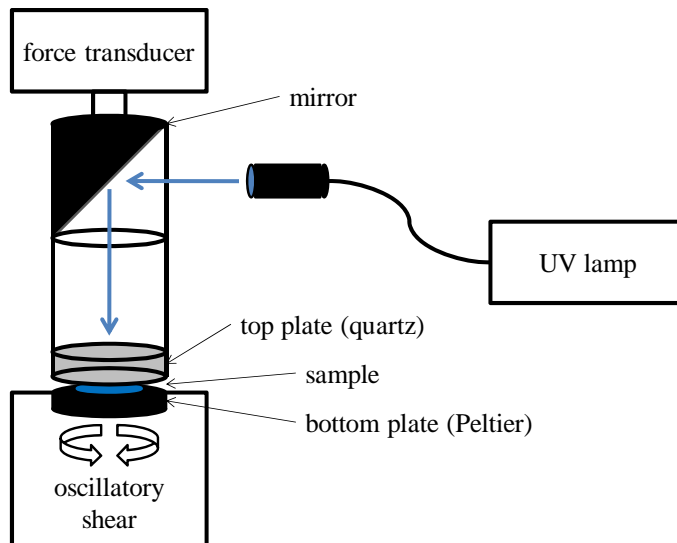


Fig. S2. Schematic of SAOS with in situ UV irradiation experimental set up.

Additionally, the rheometer's gap, and thus the sample's thickness, were easily and precisely controlled. The rheometer gap was between 0.25 and 0.28 mm for all tests studied, which is small enough for appropriate thermal equilibration and UV penetration but large enough to produce a measurable mechanical signal. Still, the transducer's signal range represented the range of accessible experimental conditions. At higher temperatures, lower frequencies, or lower strains, the torque minimum of the transducer was approached or passed, and at lower temperatures, higher frequencies, or higher strains, excessive compliance was approached or exceeded. Excessive compliance occurs when the transducer's strain is more than 70% of the total strain, thus limiting the actual strain attained by the sample as well as adding error to the data due to the low signal coming from the sample.

### S1.2 Linear Viscoelastic Strain Regime Determination

Strain amplitude sweeps were used to establish the linear viscoelastic strain regime (LVE) of the material under the given conditions. Fig. S3 shows amplitude sweeps at a) 50 °C, b) 25 °C,<sup>†</sup> c) 5 °C, and d) 0 °C. For all cases above 0 °C, regardless of whether the UV irradiation is present,  $G''$  is constant over the entire range of strains probed, and at 0 °C,  $G''$  is relatively constant with some fluctuations due to the corresponding low strain values. As for  $G'$ , in Fig. S3a and Fig. S3b, it is also relatively constant with some fluctuations at low strains until it smooths out at moderate strains and then starts to decrease at about 2% strain in Fig. S3a and 1.5% strain in Fig. S3b. In Fig. S3c,  $G'$  is constant across all of the strains achieved by the transducer, and in Fig. S3d,  $G'$  is constant with some fluctuations up to about .084%.

<sup>†</sup> The data in b) is from a different day and with about half the sample gap as the rest of the data in the paper.

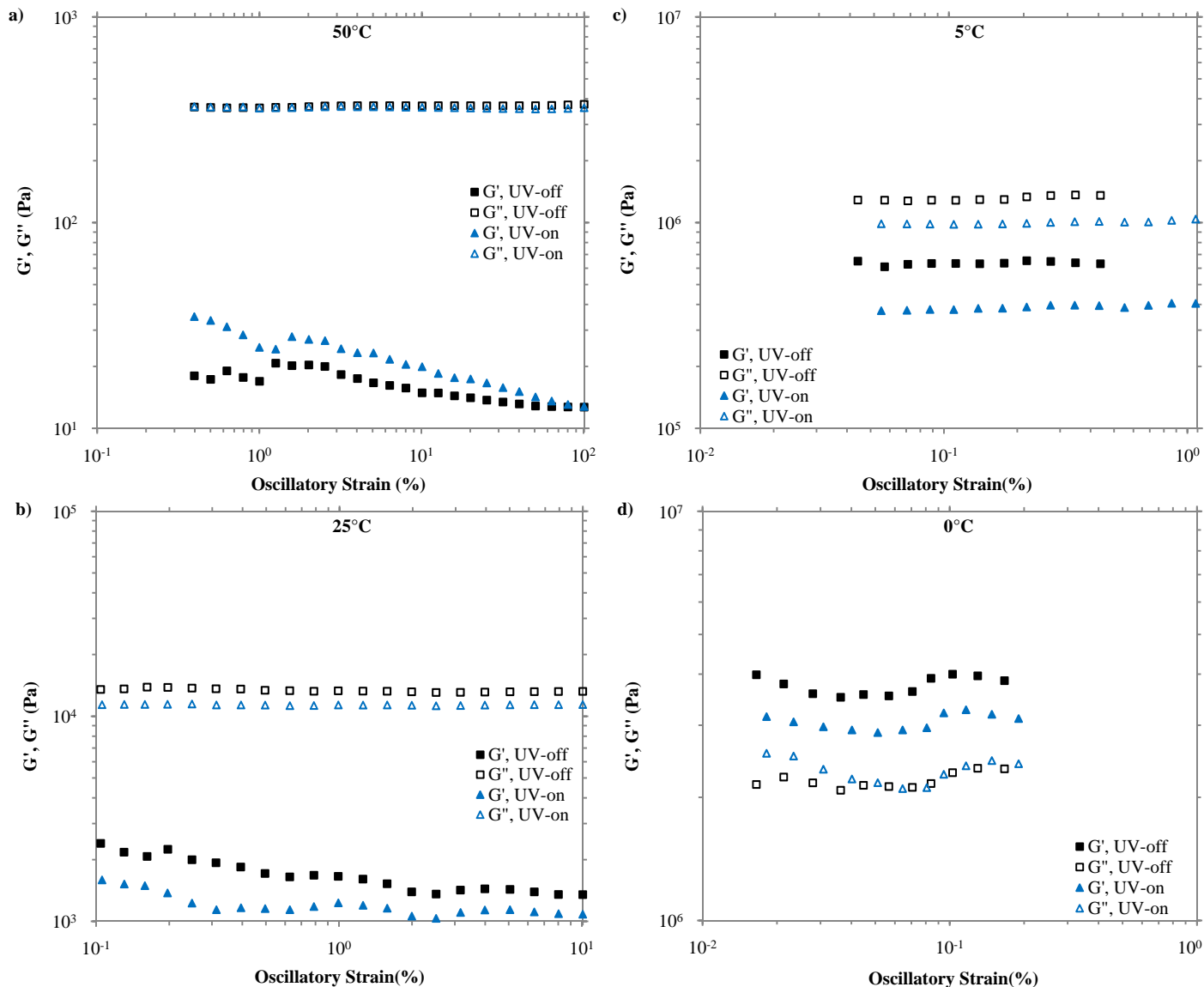
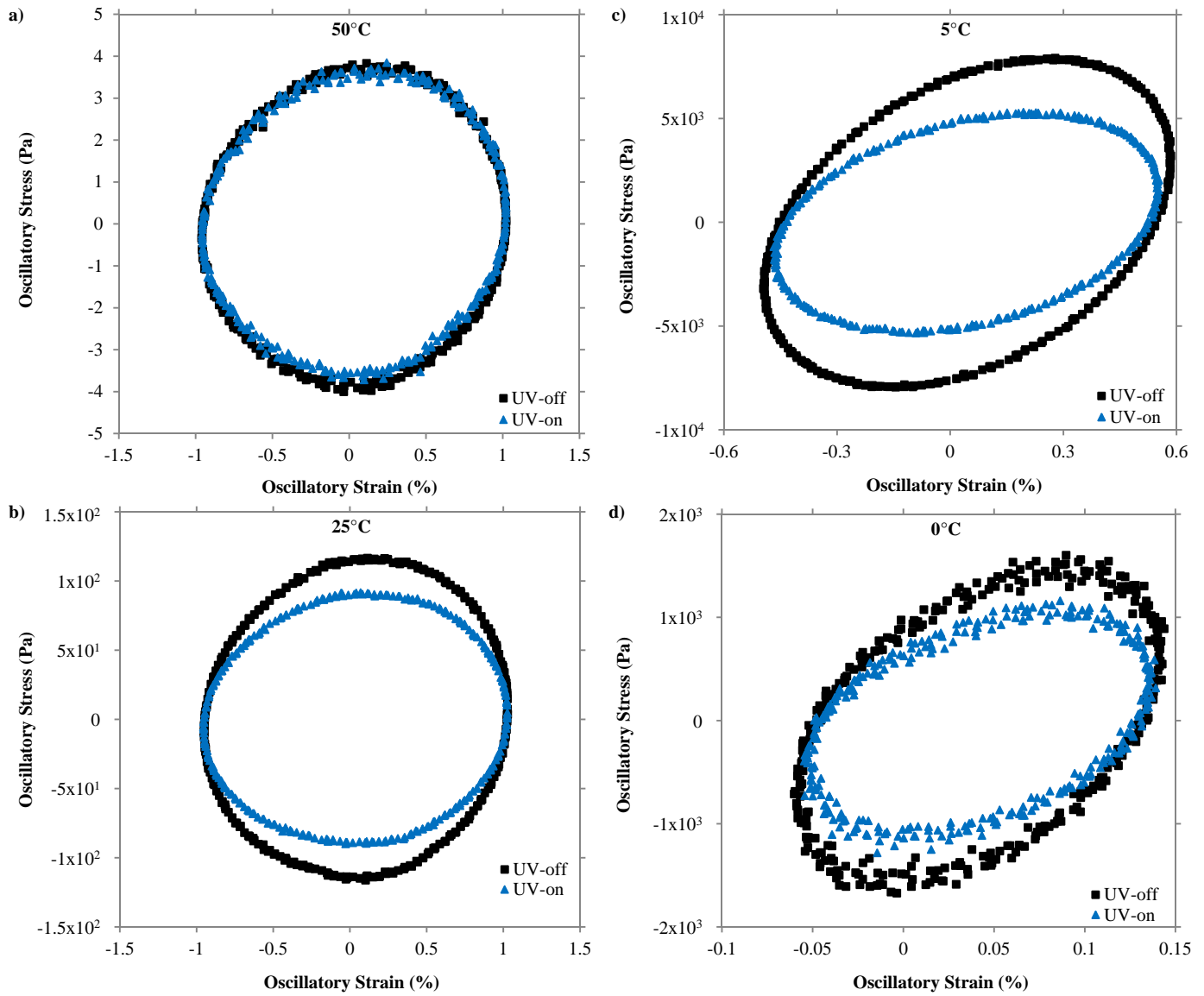


Fig. S3. Amplitude sweeps with both UV-off and UV-on at 10 rad/s and a) 50°C, b) 25°C, c) 5°C, and d) 0°C. In a), the  $G''$  values for UV-off are covered by those for UV-on because they are very close.

From the amplitude sweeps, the LVE regime was established, and linearity in  $G'$  and  $G''$  was confirmed with the Lissajous plots in Fig. S4. Fig. S4a was at 50°C and 1% commanded strain, Fig. S4b was at 25°C and 1% commanded strain, Fig. S4c was at 5°C and .437% commanded strain, and Fig. S4d was at 0°C and .084% commanded strain. Under all of the conditions tested and for both UV-off and UV-on, the Lissajous plots were elliptical, which is more

evidence that the material is, in fact, in the LVE regime. Furthermore, the plots in Fig. S4a and Fig. S4b are dominated by the viscous component, that is they are mostly round and show little linear character. The plots in Fig. S4c and, even more so, in Fig. S4d have a strong elastic component, that is the ellipse is tilted from the strong linear contribution.



**Fig. S4.** Lissajous Plots for both UV-off and UV-on at 10 rad/s and a) 50°C, b) 25°C, c) 5°C, and d) 0°C. Their elliptical forms in all of the plots are evidence that the material is in the LVE strain regime.